Available online at www.sciencedirect.com
ScienceDirect
Earth and Planetary Science Letters 259 (2007) 171–185
EPSL
www.elsevier.com/locate/epsl

The tracing of riverine U in Arctic seawater with very precise $^{234}U/^{238}U$ measurements

M.B. Andersen [a,b,*], C.H. Stirling [a,c], D. Porcelli [d], A.N. Halliday [a,d], P.S. Andersson [e], M. Baskaran [f]

[a] *Department of Earth Sciences, ETH-Zürich, Switzerland*
[b] *Department of Earth Sciences, University of Bristol, United Kingdom*
[c] *Department of Chemistry, University of Otago, Dunedin, New Zealand*
[d] *Department of Earth Sciences, University of Oxford, United Kingdom*
[e] *Laboratory for Isotope Geology, Swedish Museum for Natural History, Sweden*
[f] *Department of Geology, Wayne State University, Detroit, USA*

Received 30 October 2006; received in revised form 19 April 2007; accepted 26 April 2007
Available online 8 May 2007
Edited: H. Elderfield

Abstract

The riverine flux of U that enters the deep oceans is not well constrained since the net losses during estuarine mixing are difficult to quantify. Riverine-dissolved U normally has a higher $^{234}U/^{238}U$ activity ratio ($^{234}U/^{238}U_{ar}$) than the uniform value that characterizes open ocean seawater and could be used as a tracer of riverine inputs if one could resolve subtle variations in seawater composition. Using new mass spectrometry techniques we achieve a long-term reproducibility ±0.3‰ on $^{234}U/^{238}U_{ar}$ which permits the tracing of riverine U in seawater samples from the Arctic – a partially restricted basin that is ideal for such a study. We find that surface waters from the Arctic basins carry elevated $^{234}U/^{238}U_{ar}$ when compared with deep ocean seawater. Samples from the Canada Basin have a significant freshwater component and provide evidence that the Mackenzie River loses ~65% of its U in the Mackenzie shelf/estuary zone before entering the deeper basin. This is in contrast to samples from the Makarov Basin, which provide evidence that all of the freshwater input is derived from the major Yenisey River alone, despite the proximity of the Lena and Ob Rivers. The differing behaviour of U between the Mackenzie and Yenisey Rivers is most likely a consequence of the strong binding of U to dissolved organic matter (DOC) or secondary phases in these rivers. The Yenisey River appears to transport the majority of the DOC through the shelf and into the Makarov Basin. In contrast, the Mackenzie River appears to lose a significant amount of DOC (>50%) in the estuary/shelf zone, which may lead to loss of associated U. These findings offer a more detailed picture of the fresh riverine water flow patterns in the Arctic Ocean when compared to other geochemical proxies. The non-conservative behaviour of U in the Mackenzie River through the shelf/estuaries has important implications for U input into oceans and the total marine budget.

Keywords: Arctic Ocean; U-series; radionuclides; uranium; non-conservative; uranium disequilibrium

1. Introduction

The Arctic Ocean is an area of great significance for global climate. Much of the Arctic Ocean is presently

* Corresponding author. Department of Earth Sciences, University of Bristol, UK. Tel.: +44 117 954 5235; fax: +44 117 925 3385.
E-mail address: morten.andersen@bris.ac.uk (M.B. Andersen).

0012-821X/$ - see front matter © 2007 Elsevier B.V. All rights reserved.
doi:10.1016/j.epsl.2007.04.051

covered by a persistent perennial multiyear ice pack. It also receives a substantial input of freshwater from several major Russian and North American rivers, representing ~10% of the global river discharge into 1% of the global ocean volume. This occurs annually over a narrow time window; more than 90% of this discharge is received over an interval of 2 months. The water mass flow patterns are very complex in the Arctic Ocean, especially in the upper water layers down to a water depth of ~100 m, which represent a mixing zone between Pacific and Atlantic Ocean seawater, riverine inputs, ice melt-water and brine formation (Karcher and Oberhuber, 2002).

The extent of sea ice melting and freezing not only affects the freshwater distribution but also affects the Earth's radiation balance due to the high albedo of sea ice. There is increasing evidence that the ice covering the Arctic Ocean is more unstable at the present time, which has been attributed to global warming (Overpeck et al., 2005; Nghiem et al., 2006). Such warming has increased the riverine input into the Arctic Ocean from the major Russian rivers during the last half century (Peterson et al., 2002). This affects the mixing between freshwater sources and saline ocean water masses and has climatic implications, not only locally for the Arctic area, but also for global water mass flow patterns, such as the deep convection of the Atlantic and Pacific Ocean water masses. In particular, the stability of the Arctic Ocean has a direct bearing on the formation of thermohaline circulation and flow patterns of North Atlantic Deep Water (NADW) (Peterson et al., 2002; Ekwurzel et al., 2001; Schlosser et al., 1995; Anderson et al., 2004) and changes in the thermohaline regime can have a profound impact on global climate.

Water mass flow patterns in the Arctic Ocean are complex and numerous studies have attempted to unravel the movements in the Arctic Ocean using proxies such as salinity, $\delta^{18}O$ (defined as the permil deviation in $^{18}O/^{16}O$ away from the composition of a standard), $^{230}Th/^{231}Pa$, PO_4 content, Ba concentration and total alkalinity (Ekwurzel et al., 2001; Anderson et al., 2004; Edmonds et al., 2004; Guay et al., 2001; Schlosser et al., 1994a,b). Some of these proxies can be used to trace general freshwater flow patterns and offer the potential to separate ice melt-water from riverine inputs, although all have some limitations as well.

Marine $^{234}U/^{238}U$ activity ratios ($^{234}U/^{238}U_{ar}$) and U concentration data offer the potential to understand the distribution of freshwater inputs in greater detail and distinguish different riverine sources. The open oceans have a $^{234}U/^{238}U_{ar}$ that is consistently enriched in ^{234}U by ~15% with respect to radioactive secular equilibrium (Robinson et al., 2004a; Chen et al., 1986; Delanghe et al., 2002). It is common practice to reformulate $^{234}U/^{238}U_{ar}$ in δ-notation, whereby $\delta^{234}U = ([((^{234}U/^{238}U_{sample})/(^{234}U/^{238}U_{sec.eq.})]-1)\times 10^3$ and this terminology has been adopted here. The disequilibrium of $\delta^{234}U$ in ocean waters is mainly a direct consequence of α-recoil (Kigoshi, 1971) occurring during continental weathering, whereby the daughter ^{234}U nuclide, with a half-life of 245 thousand years (kyr) (Cheng et al., 2000), is preferentially released into the hydrological environment with respect to its ^{238}U parent (Kigoshi, 1971), resulting in highly elevated $\delta^{234}U$ (e.g., >200‰) in continental waters (Chabaux et al., 2001, 2003; Vigier et al., 2001). Uranium has a long residence time in the oceans, so that seawater has both a lower $\delta^{234}U$ value, due to the decay of the excess ^{234}U, and a U concentration that is an order of magnitude higher (Chabaux et al., 2003; Dunk et al., 2002; Palmer and Edmond, 1993).

Since the residence time of U (200–400 kyr) is substantially longer than the global ocean mixing time (1–2 kyr), seawater in the open oceans generally has a homogeneous $\delta^{234}U$ and salinity-normalised U concentration (Ku et al., 1977). The calculated residence time of 200–400 kyr is based upon estimates of global inputs, with rivers as the major source (Chabaux et al., 2003; Dunk et al., 2002; Ku et al., 1977; Henderson, 2002; Klinkhammer and Palmer, 1991). The outputs are dominated by anoxic sediments and the radioactive decay of ^{234}U (Chabaux et al., 2003; Dunk et al., 2002; Ku et al., 1977; Henderson, 2002). However, the total marine U budget is not well constrained due to large uncertainties in the input and output parameters (Chabaux et al., 2003; Dunk et al., 2002; Henderson, 2002). During the past two decades, direct U concentration and $\delta^{234}U$ measurements of marine waters have been conducted using thermal ionization mass spectrometry (TIMS) and multiple-collector inductively coupled mass spectrometry (MC-ICPMS) (Robinson et al., 2004a; Chen et al., 1986; Delanghe et al., 2002). The published data for open ocean seawater suggests that the open ocean $\delta^{234}U$ has remained constant, with no measurable variation at the permil-level (Robinson et al., 2004a; Chen et al., 1986; Delanghe et al., 2002). Prior to this study, the most precise measurements of open Atlantic seawater have given $\delta^{234}U$ of 146.6± 1.2‰ (2σ) (Robinson et al., 2004a).

The $\delta^{234}U$ activity ratio of the oceans is believed not to have varied significantly from the present-day value of ~147‰ (Robinson et al., 2004a; Chen et al., 1986; Delanghe et al., 2002) at any time throughout the last 400 ka (<±20‰) (Chabaux et al., 2003; Henderson,

2002; Hamelin et al., 1991), suggesting that very large and prolonged changes in the input and output fluxes on the marine U budget have not occurred within this time span (Chabaux et al., 2003). However, more recent studies suggest that the open ocean $\delta^{234}U$ can change on glacial–interglacial time scales (Dunk et al., 2002; Cutler et al., 2004; Robinson et al., 2004b; Esat and Yokoyama, 2006). Data from U-series dating of fossil corals suggests that the seawater $\delta^{234}U$ was up to ~15‰ lower within the last glacial period compared with the two latest interglacials (Esat and Yokoyama, 2006). Esat and Yokoyama (2006) suggest that this is due to the greater removal of estuarine U (with high $\delta^{234}U$) under reducing conditions during interglacial sea level high-stands. These authors argue that during periods of lower sea level and glacial conditions, the stored estuarine U pool becomes oxidised under atmospheric conditions, and is then mobilized and transported to the oceans during a short time-span when sea levels rise again during the following glacial–interglacial transition, thereby increasing the marine $\delta^{234}U$ (Esat and Yokoyama, 2006). One of the critical factors determining the oceanic U budget both at present and during past glacial cycles is the extent to which U is removed from the water column in estuaries. While conservative behaviour of U has been reported for some localities, such as western India (Borole et al., 1982), non-conservative behaviour has been reported at other localities, such as the Amazon River and the Kalix River entering the Baltic Sea (Swarzenski et al., 1995, 2003, 2004; McKee et al., 1987; Barnes and Cochran, 1993; Porcelli et al., 2001). Both decreases and increases in U concentration have been reported to occur in this transfer zone, as a result of different absorption and release processes (Swarzenski et al., 2003; McKee et al., 1987; Barnes and Cochran, 1993; Swarzenski and Baskaran, 2006; Breckel et al., 2005) although in general there appears to be a net loss (Barnes and Cochran, 1993).

The concentration of U and $\delta^{234}U$ can be used together to identify processes occurring in these transfer zones because open oceans and rivers differ in their $\delta^{234}U$ compositions (Swarzenski et al., 2004; Andersson et al., 1995). The Arctic Ocean shows salinity differences in surface seawater in the deeper basins (Fig. 1) so that $\delta^{234}U$ compositions and U concentrations can be used to de-convolute and quantify the processes by which amount the riverine U extend into the deeper Arctic Ocean basins beyond the estuary/shelf mixing zones. The low U concentrations in river waters, as compared to open ocean waters, makes high-precision $\delta^{234}U$ measurements essential for obtaining critical observational data, because the higher concentration of U in the ocean dominates the total U budget. However, obtaining precise and accurate measurements of $^{234}U/^{238}U$ is extremely difficult due to the large difference in the relative abundance of these two isotopes ($\sim 10^{-4}$ range).

Here we present $\delta^{234}U$ measurements acquired with unsurpassed levels of precision and coupled U concentration data for a suite of water samples from the Arctic Ocean and adjoining major rivers in North America (Mackenzie) and Siberia (Lena, Ob and Yenisey), and are able to detect sub-permil variations in $\delta^{234}U$. The high precision of these measurements provide the opportunity for studying the behaviour of U transported into the Arctic Ocean, and the potential to trace distinct riverine inputs into the Arctic region from closely situated major rivers.

2. Materials and methods

2.1. Samples

Arctic Ocean seawater and the Mackenzie, Lena, Yenisey and Ob Rivers were sampled and measured for $\delta^{234}U$ and U concentration by multiple-collector inductively coupled plasma mass spectrometry (MC-ICPMS) (Figs. 1 and 2). Measurements of $\delta^{18}O$ were performed on selected samples. All seawater samples were collected from deep ocean basins, with the exception of sample AWS-2000 Station 5, which was collected at the shelf break.

Samples numbered 1 to 30 were collected along the Leg II transect from Svalbard to the Makarov Basin during the Swedish Arctic Ocean expedition AO-01 in 2001 using the icebreaker *Oden*. A hydrological description of the LEG II sampling profile can be found in Björk et al. (2002). The LEG II transect samples were collected at a water depth of 8 m using the *Oden* seawater intake, which is constructed with polyethylene tubing. During the same expedition, a depth profile extending from the surface down to a water depth of 2500 m was collected from the Makarov Basin. The deep-water samples were collected using a CTD-rosette equipped with 60 L, 30 L and 20 L GO-FLO® samplers. All water samples were filtered using silicone tubing and a peristaltic pump through a 0.22-μm filter (142-mm diameter nitrocellulose membrane filter) mounted in a polycarbonate filter holder.

In the Canada Basin, samples from Station 5 from the continental rise (73°15′N; 155°69′W) and Stations 3 and 4 in deep basin (75°13′N; 149°54′W) were collected during the USCGC Polar Star expedition AWS-2000, carried out in the summer of 2000. The

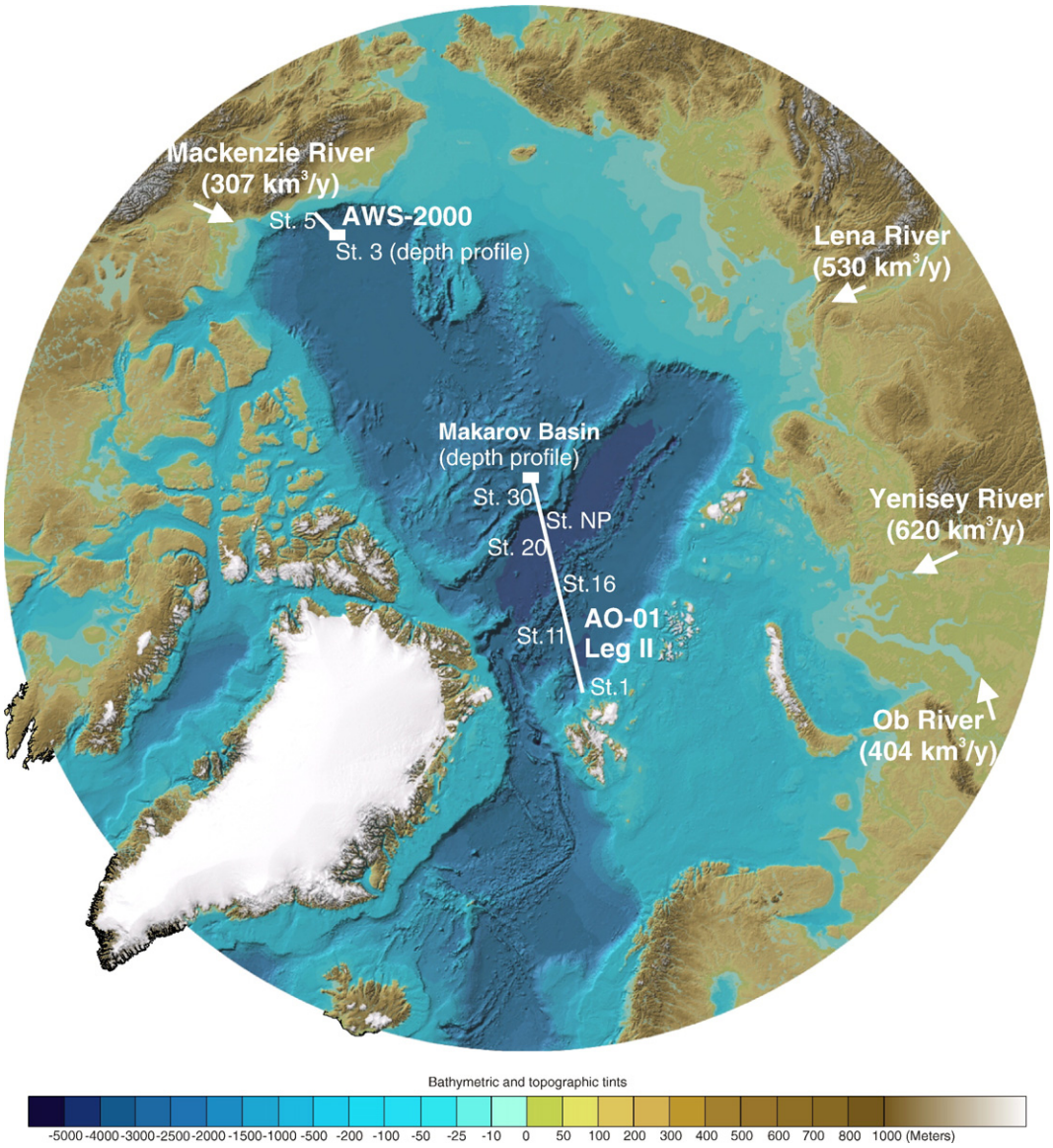

Fig. 1. Bathymetric map of the Arctic area showing the seawater sampling positions in (1) the Canada Basin (AWS-2000), where samples were collected along a transect in 5-m water depth and along a depth profile located at Station 3; and (2) The Makarov Basin (AO-01, Leg II), where surface water samples were collected from a water depth of 8 m along a transect extending from Svalbard to the North Pole, and along a depth profile located at Station 30 in the Makarov Basin. The three major Siberian Rivers, the Ob, Lena and Yenisey, as well as the North American Mackenzie River, were also sampled. The annual average water discharge from each river is given in brackets (from Holmes et al., 2002). The bathymetric map was sourced from International Bathymetric Chart of the Arctic Ocean (IBCAO); http://www.ngdc.noaa.gov/bathymetry/arctic/arctic.html.

Canada Basin samples include a surface transect, collected in a water depth of 5 m, and a deep-water profile at Station 3, extending from the surface down to a depth of 3000 m. Further details for the AWS-2000 samples can be found in Trimble et al. (2004). All samples were filtered in the field using a 0.45-μm particle size cut-off and acidified onboard.

The river water data presented here were collected as part of the PARTNERS (Pan-Arctic River Transport of Nutrients, Organic Matter and Suspended Sediments) project in 2003 from the Mackenzie, Lena, Yenisey, and Ob Rivers. Samples were collected near river mouths (above tidal influence) in order to obtain fully integrated watershed signals and the most relevant freshwater end-member values for oceanographic tracking. Further sampling descriptions can be found on the PARTNERS project website: http://www.ecosystems.mbl.edu/partners/ and in Cooper et al. (2005).

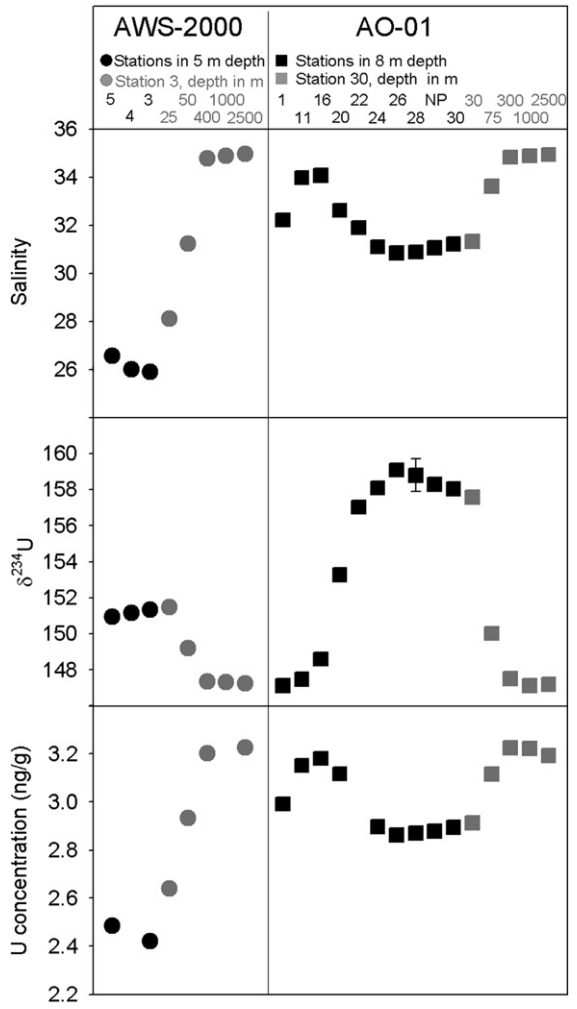

Fig. 2. The spatial and depth distribution of the $\delta^{234}U$ and U concentration of the measured samples from AWS-2000 (Canada Basin) and AO-01 (Central Arctic Basins). Black symbols symbolise samples collected from horizontal surface profiles, and grey symbols represent the depth profile at each locality. 2σ error bars are plotted and are generally smaller than the size of the symbols.

2.2. $^{234}U/^{238}U$ measurements

Uranium in each of the water samples was co-precipitated with Fe using standard methods (Chen et al., 1986). Subsequent ion exchange column chemistry was performed using TRU-spec ion exchange resin to extract the U from the sample matrix, and an additional purification step was then carried out using U-TEVA-spec ion exchange resin (both sourced from Eichrom) (Potter et al., 2005; Luo et al., 1997). Total procedural blanks correspond to <2 pg of ^{238}U and were negligible. All measurements were performed using a Nu Instruments Nu Plasma MC-ICPMS at the ETH, Zürich. The majority of the $^{234}U/^{238}U$ measurements were performed using methods described in Andersen et al. (2004) and a configuration of multiple-Faraday cups (F–F) in place of the conventional Faraday–electron multiplier configuration (F–M) adopted in previous studies.

The F–F protocol takes advantage of a 10^9 Ω positive feedback resistor coupled to the ^{238}U Faraday cup instead of the standard 10^{11} Ω resistor. This allows an ion beam that is 100 times larger than usual to be placed in the ^{238}U Faraday cup, thus expanding the dynamic range of the Faraday collector array to the 10^5 level, as required for $^{234}U/^{238}U$ measurement, and allowing the simultaneous measurement of ^{238}U ($\sim 9\times 10^{-9}$ A), ^{235}U ($\sim 7\times 10^{-11}$ A) and ^{234}U ($\sim 5\times 10^{-13}$ A) in the same analysis sequence (Andersen et al., 2004, submitted for publication). Electronic background noise is monitored for 75 s initially, by deflecting the ion beams away from the axial optical plane. The analyte solution, containing 2–3 ppm U, is then introduced and on-peak data are acquired over a 2-min acquisition period. Significant tailing of the large ^{238}U beam below the ^{234}U isotope is corrected for by normalization to a CRM-145 U metal bracketing standard, assuming an identical ^{238}U tailing behaviour for both the sample and standard (Andersen et al., 2004). The long-term reproducibility obtained with this technique, as documented using the chemically purified Harwell uraninite standard (HU-1), as well as in-house uraninite (CZ-1) and coral (HIBC) standards, was ±0.31‰ (2σ) or better over an extended period of 2 years (Andersen et al., 2004, submitted for publication). Repeat measurements of Arctic seawater, sampled from transect AWS-2000 Station 3, 5 m, yielded a similar long-term reproducibility value ±0.28‰ at the 2σ level (Fig. 3). Each measurement consumes ~500 ng of U, equivalent to the amount extracted from 200–300 ml of seawater.

Several samples were also measured conventionally using a mixed-mode F–M array and sample-standard bracketing techniques reported in Andersen et al. (2004). Although less precise, this method requires a smaller load size corresponding to ~50 ng of U, and is ideal when sample size is limited. These conventional F–M measurements were conducted as a single static cycle by monitoring the minor ^{234}U ion beam in a secondary electron multiplier (SEM) equipped with an ion counter and retardation filter. The Faraday-multiplier gain is determined using bracketing measurements of CRM-145, measured at a similar intensity as the unknown sample (^{238}U $\sim 1.5\times 10^{-10}$ A). All F–M measurements were performed over 40 cycles with signal integration times of 5 s. Total acquisition times

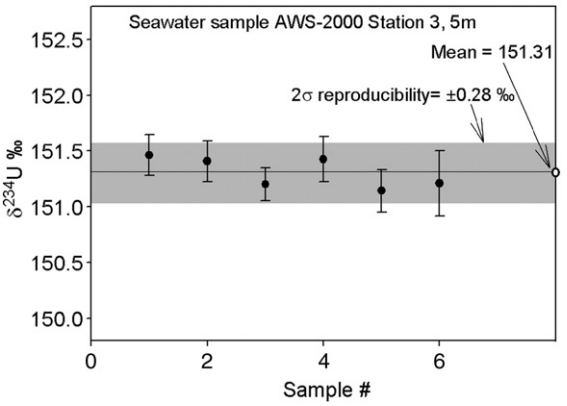

Fig. 3. Repeat δ^{234}U F–F measurements of the seawater sample AWS-2000 Station 3, 5-m depth, yielding a mean value of 151.3±0.1 ($2\sigma_m$, $n=6$) and an external reproducibility of ±0.28‰ (2σ), similar to the long-term reproducibility exhibited by standards measured using this method (Andersen et al., 2004, in review). Measurements were conducted during independent sessions conducted over an extended period of 6 months for two independently processed aliquots.

were ~8 min (including the measurement of the background zeroes at half-mass locations) (Andersen et al., 2004). Consecutive measurements of CZ-1 are identical, within error, to those obtained using the F–F method and yielded a value for long-term reproducibility of ±0.9‰ (2σ). All water samples analyzed using the F–M method have similar associated uncertainties.

All measurements of ^{234}U/^{238}U were corrected internally for instrumental mass fractionation during the course of the measurement by normalizing the measured ^{238}U/^{235}U against the true value using the exponential mass fractionation law (Hart and Zindler, 1989). It is usual to assume that ^{238}U/^{235}U has a uniform ratio of 137.88 throughout the Earth, although using double spiking techniques (Stirling et al., 2005, 2006) it has been shown that low-temperature terrestrial samples show natural variations of up to 1.3‰ (Stirling et al., 2003, in press). In studies by Andersen et al. (submitted for publication) and Stirling et al. (in press) the ^{238}U/^{235}U of the CRM-145 and HU-1 standards, as well as selected samples of Pacific island coral and oceanic seawater, were measured to high levels of precision with associated uncertainties of ±0.1‰, using protocols reported in Stirling et al. (2005, 2006). Measurements for the seawater and corals are identical, within analytical error, and are marginally offset by 0.1‰ from HU-1, and significantly offset from CRM-145 by ~0.5‰ (Andersen et al., submitted for publication; Stirling et al., in press).

Activity ratios for ^{234}U/^{238}U were calculated by normalization against the secular equilibrium standard HU-1, measured in a similar fashion as the seawater samples (Andersen et al., submitted for publication; Stirling et al., in press), and adopting the ^{234}U half-life determined by Cheng et al. (2000). This implies that provided HU-1 is in secular equilibrium with respect to ^{234}U and ^{238}U, only the magnitude of the ^{238}U/^{235}U offset between HU-1 and the analyzed samples is critical for the accuracy of the ^{234}U/^{238}U measurements, and that the assumed "true" value adopted for the ^{238}U/^{235}U normalization (in this case 137.88) is not important. Variation of ^{238}U/^{235}U between sample and standards and HU-1 (assumed to be 137.88) has been incorporated into the mass bias correction for all ^{234}U/^{238}U measurements, assuming that the Arctic seawater and the river samples all have a similar ^{238}U/^{235}U composition as oceanic seawater. The ^{238}U/^{235}U of HU-1 and the seawater samples are nearly identical, and only a marginal ^{238}U/^{235}U offset correction for the calculated δ^{234}U were needed for these, whereas CRM 145 yields a δ^{234}U of −36.90±0.08‰ ($2\sigma_m$, $n=14$), as apposed to δ^{234}U=−36.44 in Andersen et al. (2004), with respect to HU-1 and incorporating the natural variability in ^{238}U/^{235}U into the U-series calculations.

3. Results and discussion

Uranium concentrations and δ^{234}U were determined for seawater sampled along (a) a surface transect and a depth profile from the Canada Basin, (b) a depth profile from the Makarov Basin, and (c) a surface transect (Leg II) extending from Svalbard to the North Pole (Fig. 2 and Table 1). The majority of less saline surface seawater samples have δ^{234}U values of 157‰ to 159‰ for the central Arctic (samples 26, 28, and 30) and ~151‰ for the Canada Basin. These values are consistently higher than the ~147‰ value reported for open ocean seawater. Measurements of δ^{234}U that are identical, within error, of open ocean values were found for the deeper and higher salinity (~35) seawater samples; six deep Arctic seawater samples from the Canada and Makarov Basins yield an average δ^{234}U of 147.3±0.27‰ (2σ), identical to that measured for the Atlantic Ocean of 146.6±1.2‰ (2σ) by Robinson et al. (2004a).

3.1. Arctic rivers

The Siberian river samples have relatively low U concentrations of <0.25 ng/g but elevated δ^{234}U of ~600–1600‰ (Fig. 4). In contrast, the North American Mackenzie River has a δ^{234}U of ~385‰ and U concentration of ~0.64 ng/g, similar to values reported

Table 1
Water samples

Sampling station		Depth (m)	$\delta^{234}U$ (‰)[a]	±2σ	U (ng/g)	±2σ[b]	Salinity[c]	$\delta^{18}O$ (‰)[d]	±2σ
AWS-2000 (Canada Basin)									
5	73°15′N 155°60′W	5	150.9	0.3	2.49	0.01	26.56	−3.38	0.12
4	73°50′N 152°55′W	5	151.2	0.3			26.01		
3	75°13′N 149°54′W	5	151.3	0.3	2.42	0.01	25.90	−3.61	0.12
3		25	151.5	0.3	2.64	0.01	28.11	−3.46	0.12
3		50	149.2	0.3	2.93	0.01	31.24	−2.21	0.12
3		400	147.4	0.3	3.20	0.02	34.80	0.42	0.12
3		1000	147.3	0.3					
3		3000	147.3	0.3	3.23	0.02	34.96	0.53	0.12
AO-01 (central Arctic Basins) LEG II transect									
1		8	147.1	0.3	2.99	0.01	32.22		
11		8	147.5	0.3	3.15	0.02	33.98		
16		8	148.6	0.3	3.18	0.02	34.08		
20		8	153.3	0.3	3.12	0.02	32.63		
22		8	157.0	0.3			31.91		
24		8	158.1	0.3	2.90	0.01	31.10		
26		8	159.1	0.3	2.86	0.01	30.85		
28		8	158.8	0.9	2.87	0.01	30.90		
North pole (NP)		8	158.3	0.3	2.88	0.01	31.07		
30	Makarov Basin	8	158.0	0.3	2.90	0.01	31.23		
		30	157.6	0.3	2.91	0.01	31.33		
		75	150.0	0.3	3.12	0.02	33.62		
		300	147.5	0.3	3.22	0.02	34.84		
		1000	147.1	0.3	3.22	0.02	34.89		
		2500	147.2	0.3	3.19	0.02	34.95		
River waters									
Ob	66°31′N 66°36′E		659.8	0.9	0.124	0.001			
Lena	66°46′N 123°22′E		1256.1	0.9	0.107	0.001			
Yenisey	69°23′N 86°09′E		1591.9	0.9	0.203	0.001			
Mackenzie	67°26′N 33°45′W		384.4	0.9	0.638	0.003		−19.44	0.12
Vigier et al. (2001)			*380*	*10*	*0.73*	*0.01*			

[a] $\delta^{234}U=[(^{234}U/^{238}U)/(^{234}U/^{238}U)_{eq}]-1\times10^3$. $(^{234}U/^{238}U)_{eq}$ is the atomic ratio at secular equilibrium and is equal to $\lambda_{238}/\lambda_{234}=5.4891\times10^{-5}$, where λ_{238} and λ_{234} are the decay constants for ^{238}U and ^{234}U, respectively, adopting the ^{234}U half-life of Cheng et al. (2000). Errors are representative of the 2σ long-term reproducibility of the U isotopic standards and are ±0.3‰ for the F–F and ±0.9‰ with the F–M techniques, respectively. All activity ratios are calculated by normalization to HU-1, assuming HU-1 is in secular equilibrium with respect to ^{234}U and ^{238}U (see also Andersen et al., submitted for publication). For all isotope ratios, the measurement errors ($2\sigma_m$) for HU-1 were incorporated into the uncertainties quoted for the unknown samples.

[b] Uranium concentration measurements were obtained from ~10 ml and ~40 ml aliquots of each of the seawater and river water samples, respectively. Each aliquot was spiked with a ^{233}U–^{236}U tracer to obtain a $^{238}U/^{233}U$ value of ≤1000. Samples were chemically processed through TRU-spec ion exchange columns using protocols reported in Luo et al. (1997). The extracted U was measured on the Nu Plasma MC-ICPMS using the same methodology and F–F collector configuration as reported in Andersen et al. (2004), but including an additional measurement of ^{233}U, as described in (Andersen et al., submitted for publication). Typical ^{238}U intensities of 3×10^{-10} A gave rise to internal measurement errors ($2\sigma_m$) and an external reproducibility (2σ) of ±0.6‰. Tailing from ^{238}U below mass ^{233}U, characterized by monitoring an unspiked CRM 145 standard prior to the introduction of spiked samples, was determined to be 0.17±0.03 ppm. This tailing contribution, as well as the trace quantities of natural ^{238}U and ^{235}U present in the artificial spike (Andersen et al., submitted for publication), was corrected for off-line. A conservative error of ±5‰ (2σ) was assigned to the U concentration measurements by taking into consideration the weighing error as the dominant source of uncertainty.

[c] Salinities were measured on site. See Björk et al. (2002) and Trimble et al. (2004).

[d] Defined as the permil deviation in $^{18}O/^{16}O$ away from the composition of the V-SMOV standard $\delta^{18}O=\{[(^{18}O/^{16}O)/(^{18}O/^{16}O)_{v\text{-}smov}]-1\}\times10^3$. Measurements of $\delta^{18}O$ were performed on 8–10 ml aliquots of the seawater and river water samples at the Stable Isotope Lab INSTAAR at the University of Colorado, using a Micromass SIRA Series II Dual Inlet mass spectrometer. Results are reported relative to V-SMOW (‰). Standards were reproducible to ±0.12‰ (2 s) during the period these measurements were conducted. Further information on the methods utilized can be found at the INSTAAR website: http://mysticplum.colorado.edu/groups/sil/analyses.

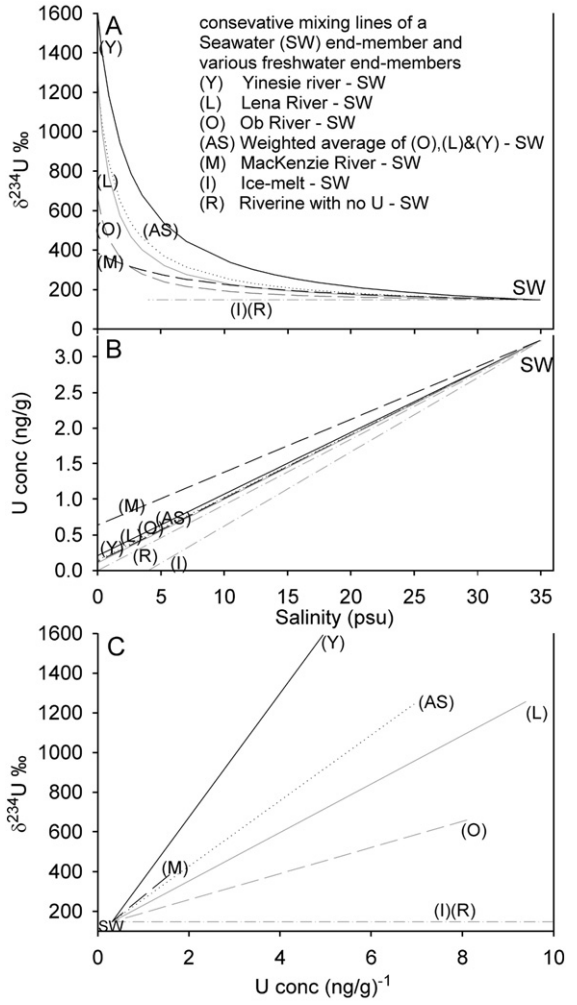

Fig. 4. Plots of (A) δ^{234}U versus salinity, (B) U concentration versus salinity, and (C) δ^{234}U versus U concentration. Calculated two-component mixing lines are shown: The saline end-member (SW) is based upon the composition, determined in this study, for deep seawater samples (at >250-m water depth). The freshwater end-members are the (Y) Yenisey, (L) Lena, and (O) Ob Rivers, (AS) a weighted average of these three Siberian river sources, (M) the Mackenzie River, (I) ice melt-water, with an assumed salinity of 4 (Ekwurzel et al., 2001), and (R) a riverine component with a salinity of 0 and containing no U.

in Vigier et al. (2001) taken several years prior to the river sample measured in this study (Table 1). Riverine U isotopic compositions and concentrations can potentially vary on a seasonal and yearly scale, as has been observed at some other localities, such as the boreal subarctic Kalix River in northern Sweden (Andersson et al., 1998, 2001; Porcelli et al., 1997). The Kalix River exhibits only marginal variability in U concentration (<10%) but larger variability in δ^{234}U (480‰ to 960‰), with the highest δ^{234}U corresponding to episodes of peak discharge (Andersson et al., 2001). The potential seasonal variability in δ^{234}U for the Arctic rivers investigated in the present study is unlikely to be significant due to the short time-span (2–3 months per year) during which they are flowing into the Arctic Ocean together, as well as homogenisation of the isotopic signature due the large drainage area inherent to each river system. Variability in uranium concentration could potentially occur due to differing degrees of snow melt addition, for example. In the following sections, the measured U concentration and δ^{234}U are adopted as the end-member composition for each river. Although these values are based on one measurement per river, potential annual and seasonal variability in the riverine U concentration and δ^{234}U is taken into consideration in the discussion.

The concentration of major cations (Na+Ca+K+Mg) and dissolved organic carbon (DOC) values for each of the sampled river waters are summarized in Table 2. The annual water discharge and suspended particle flux are also included. It is important to note that the Mackenzie River differs significantly from the Siberian Rivers, in that it contains a lower DOC concentration but a larger suspended sediment flux (Cooper et al., 2005; Holmes et al., 2002). A significant positive correlation between DOC and U concentration has been observed in other marine systems (Chabaux et al., 2003; Mann and Wong, 1993). This is not observed in the present study, in fact the Mackenzie River has the highest U concentration but the lowest DOC. Furthermore, a positive correlation between the concentrations of major cations and U has been found in compiled data sets of several riverine systems (Borole et al., 1982), but this is not found in our data for four Arctic river samples. The Mackenzie River is characterized by both a higher U concentration and major cation content than the Siberian Rivers, while the Yenisey River has the highest U concentration but the lowest major cation content compared to the Lena and Ob Rivers (Table 2).

3.2. Canada Basin (AWS-2000)

The Canada Basin surface transect (AWS-2000, 5 m depth) samples exhibit the lowest salinities (<27) and the highest δ^{234}U (~151‰) values, whereas seawater sampled from water depths below 300 m have δ^{234}U approaching ~147‰. Uranium concentrations vary from ~2.42 ng/g for surface water samples to ~3.23 ng/g for deep-water samples. Salinities, U concentrations and δ^{234}U compositions for the Canada Basin seawater samples are plotted in Fig. 5. Calculated

Table 2

River	MAD [a] (km^3/yr)	DOC [b] (±1σ) (μmol)	SPF [c] ($\times 10^6$ metric tons/yr)	MC [d] (mg/L)	U [e] (±2σ) (ng/g)
Mackenzie	307	375 (100)	124	49.9	0.638 (0.003)
Lena	530	724 (283)	20.7	37.0	0.107 (0.001)
Ob	404	733 (167)	15.5	32.8	0.124 (0.001)
Yenisey	620	733 (316)	4.7	23.3	0.203 (0.001)

[a] Mean annual discharge; data from Holmes et al. (2002).
[b] Dissolved organic carbon; data from Cooper et al. (2005).
[c] Suspended particle flux; data from Holmes et al. (2002).
[d] Major cations (Na+Ca+K+Mg); data from PARTNERS (http://www.ecosystems.mbl.edu/partners/).
[e] Uranium concentrations; this study from Table 1.

two-component mixing lines, based on seawater (SW) as one end-member component and ice melt-water or the Mackenzie River composition as the other, are also displayed in Fig. 5. A SW–Lena River mixing line is also shown because the Lena River can also be a freshwater component in the Canada Basin, although the SW–Lena mixing line does not differ significantly from the Mackenzie River–SW mixing line. The measured seawater compositions plot within a mixing area defined by the two ice melt–SW and Mackenzie River–SW mixing lines. This could reflect a three-component mixing zone, whereby the freshwater component consists of both ice melt and Mackenzie River water. An alternative possibility is that the composition of the Mackenzie River has been modified by ~65% loss of its U in the estuary/shelf zones before entering the deeper Canada Basin. A third modelled mixing line based on this ~65% U loss and degrees of ice melt effect on the freshwater composition is also displayed in Fig. 5.

Distinguishing between these two scenarios is not possible using salinity, δ^{234}U and U concentration data alone. However, δ^{18}O is a good water mass tracer because the saline Atlantic and Pacific waters have significantly different δ^{18}O compositions than the major rivers entering the Arctic Ocean, which again differ in their δ^{18}O signature from fresh ice melt-water (Ekwurzel et al., 2001). Thus, a plot of δ^{18}O versus salinity is generally able to distinguish riverine water masses from ice melt and saline ocean waters in the Arctic Ocean (Ekwurzel et al., 2001; Schlosser et al., 1994b; Macdonald et al., 1999). δ^{18}O was measured on selected samples from the Canada Basin and the Mackenzie River. A plot of δ^{18}O versus salinity is shown in Fig. 5D, together with mixing lines represented by the ice melt–SW and Mackenzie River–SW components. The data show that intermediate depth water samples (Station 3, 25 and 50 m) closely follow the Mackenzie River–SW mixing line. The two surface seawater samples (Stations 5 and 3) are also close to this line but the results provide evidence for an additional minor ice melt-water input as well (Fig. 5D). A minor ice melt input together with a riverine freshwater component has also been shown in other studies on the basis of the δ^{18}O signature of seawater in the Canada Basin (Cooper et al., 2005; Macdonald et al., 1999). Using the δ^{18}O and salinity results of this study, the ice melt contribution to the freshwater component in the 5-m depth samples at Stations 3 and 5 is estimated to be 20–40% (Fig. 5). If freshwater from ice melt is mixed with Mackenzie River water (with 65% U loss) in the above-mentioned proportion, then the fit with the measured U concentration and δ^{234}U compositions of Stations 3 and 5 at 5-m depth is very good (Fig. 5C).

This demonstrates that U in the Mackenzie River estuary is behaving non-conservatively, with significant losses of riverine U (~65%) occurring in the estuary/shelf zone. Significant variability in the δ^{234}U and U concentration for the Mackenzie River could potentially alter these conclusions, particularly if the river's typical U concentration were substantially lower than the value obtained in this study. Measurements of both δ^{234}U and U concentration acquired in the present study are in perfect agreement with those obtained several years earlier during an independent study of the same river by Vigier et al. (2001). The δ^{234}U values are ~385±1‰ versus 380±10‰ and the U concentrations ~0.64 versus 0.72 ng/g. This robust replication provides evidence that regardless of any minor seasonal variations in δ^{234}U and U concentration ~65% of uranium is lost in the estuary/shelf zone of the Mackenzie River. Additional riverine data would be desirable to explore seasonal variations in more detail however.

The behaviour of U in estuaries is complex and varies between different localities, and both conservative and non-conservative behaviour have been observed (Swarzenski et al., 2003). Non-conservative behaviour has, for example, been observed for other river–estuary systems such as the Kalix River (Andersson et al., 1995, 1998,

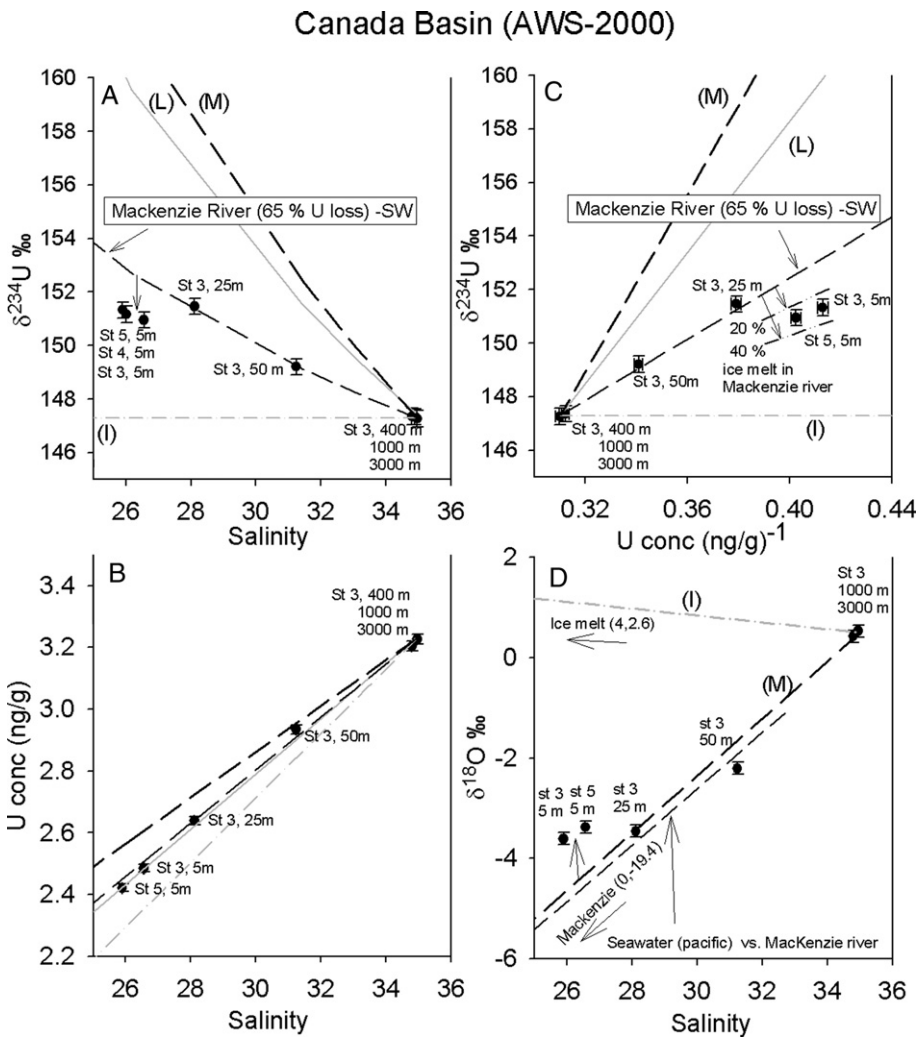

Fig. 5. Canada Basin (AWS-2000) seawater samples plotted as (A) $\delta^{234}U$ versus salinity, (B) U concentration versus salinity, (C) $\delta^{234}U$ versus the inverse U concentration and (D) $\delta^{18}O$ versus salinity. Mixing lines between a seawater end-member and (L) Lena, (M) the Mackenzie River, and (I) ice melt-water end-members are plotted, as shown in Fig. 4. A mixing line between SW and Mackenzie River, but with a 65% loss of riverine U in the shelf/estuary zone is also plotted. The intermediate samples plot along this latter mixing line, whereas the surface samples plot close to this mixing line, however they appear to contain a minor ice melt component as well. This is also suggested in (D) which shows $\delta^{18}O$ versus salinity for selected samples in the Canada Basin (AWS-2000). Here, different mixing lines are plotted; a deep seawater end-member (with a $\delta^{18}O$ of ~0.5‰) coupled to (M) a Mackenzie River and (I) an ice melt-water end-member (Ekwurzel et al., 2001). Also plotted is an assumed Pacific Ocean end-member (Ekwurzel et al., 2001), (with a different $\delta^{18}O$ composition for SW than the Atlantic Ocean) coupled to a Mackenzie River end-member. The $\delta^{18}O$ versus salinity data show that in the surface water samples, the majority of freshwater comes from the Mackenzie River but a secondary ice melt-water component is also recorded. Using the $\delta^{18}O$ and salinity data, it is possible to calculate the percentage contribution to the freshwater fraction from ice melt and Mackenzie River water (see Cooper et al., 2005). Using different end-member compositions for the seawater (Atlantic versus Pacific) about 20–40% of the freshwater component is ice melt at AWS-2000 Stations 3 and 5. This is plotted with stippled lines in C were the ice melt component is subtracted from the Mackenzie River (with 65% U loss) signature.

2001; Porcelli et al., 1997, 2001) and the Amazon Delta (Swarzenski et al., 1995, 2003, 2004) where U removal occurs. A detailed study found that low salinity U removal in the Kalix River estuary zone is likely to be a consequence of absorption onto settling flocculated colloids of organic material and Fe, with U losses occurring of up to 50% (Andersson et al., 2001).

It has been shown that colloidal U in coastal waters is strongly bound to DOC and can be removed from the water column (Chabaux et al., 2003; Swarzenski et al., 1995; Mann and Wong, 1993). The Mackenzie River contains a significant amount of DOC, with a mean concentration of 375 μM measured during 2003–2004, although the DOC of Arctic Rivers is highly variable on

a yearly scale and therefore difficult to accurately quantify (Table 2) (Cooper et al., 2005; Hansell et al., 2004). The Arctic River systems introduce a significant amount of terrestrial carbon into the Arctic Ocean (Dittmar and Kattner, 2003; Macdonald et al., 1998) but a significant loss of DOC (>50%) is believed to occur in areas of the north Canada shelf, before freshwaters reach central parts of the Arctic Basins (Cooper et al., 2005; Hansell et al., 2004). The mechanism for this loss is assumed to be microbial degradation transferring the DOC into CO_2 (Hansell et al., 2004). The Mackenzie River also has a significant annual suspended sediment flux (Holmes et al., 2002) and it is estimated that about half of the suspended particle flux is lost from the Mackenzie River delta entering the Canada Basin (Holmes et al., 2002; Macdonald et al., 1998). The substantial loss of suspended sediment phases on the shelf could potentially also scavenge U out of the water column through adsorption onto flocculating colloidal organic or Fe-coated phases, as has been observed for other estuary systems (Porcelli et al., 2001; Andersson et al., 1995, 1998, 2001; Porcelli et al., 1997).

3.3. Central Arctic basins

Results from the depth profile of the Makarov Basin and the Leg II surface transect are plotted in Fig. 6 together with calculated two-component mixing lines between a SW end-member and a riverine end-member corresponding to the weighted average of the Siberian rivers. Below a water depth of 300 m, the Makarov Basin samples reach salinities of ~35 and $\delta^{234}U$ of ~147‰. The surface samples with the lowest salinities (~28) also show the highest measured $\delta^{234}U$ (~159‰).

With only one exception, the Makarov Basin samples and those corresponding to the northern section of the Leg II surface transect (from Station 20 northwards) appear to follow a two-component mixing line between the Yenisey and SW end-member components. The data for Leg II Stations 1, 11 and 16, sampled along the southern section of this transect, are likely to have experienced other freshwater inputs aside from the Yenisey River. In particular, Stations 1 and 11 appear to have incorporated significant freshwater input from ice melt (Fig. 6). On the basis of $\delta^{18}O$ measurements, Ekwurzel et al. (2001) have argued that samples with lower salinities (<34.8) collected near Svalbard have experienced significant ice melt-water input, which could account for the open ocean water $\delta^{234}U$ observed in this study for Leg II Stations 1 and 11. Leg II Station 20, follows the Yenisey–SW mixing line in the salinity versus $\delta^{234}U$ diagram (Fig. 6A), but appears to have an elevated U concentration (~3% higher than expected) in the salinity versus U concentration diagram (Figs. 6B, C). Leg II Station 1 also has an unexpectedly high U

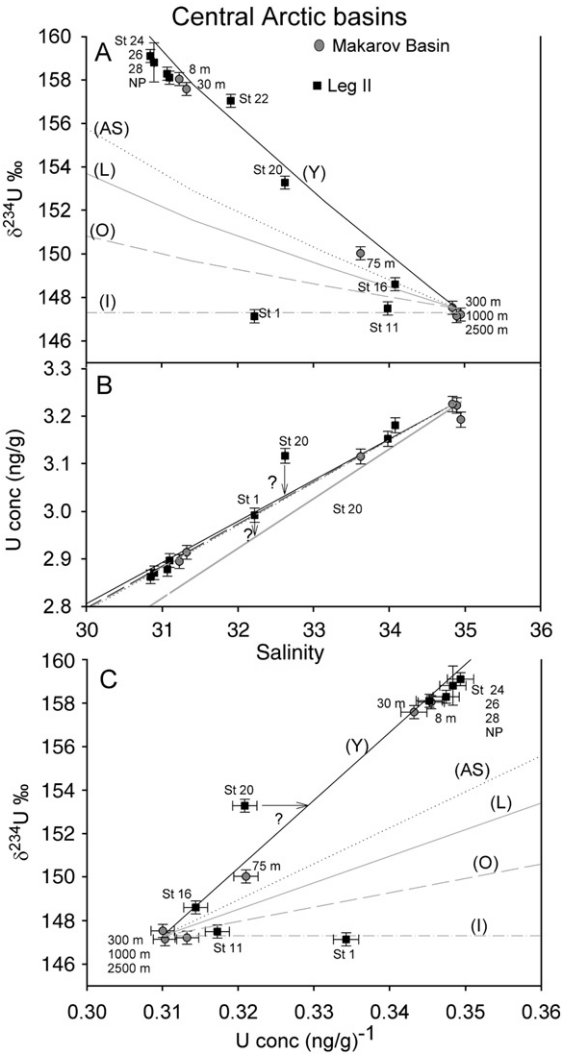

Fig. 6. The central Arctic Ocean (Leg II transect and Makarov Basin) seawater samples are plotted in terms of (A) $\delta^{234}U$ and (B) U concentration versus salinity, and (C) $\delta^{234}U$ versus the inverse U concentration. Two-component mixing lines between a seawater end-member and an end-member represented by the (Y) Yenisey, (L) Lena, and (O) Ob Rivers, (AS) a weighted average of the Russian Rivers and (I) ice melt-water are represented, as shown previously in Fig. 4. The majority of samples plot along the (Y) Yenisey–SW River mixing line, which has the most enriched $\delta^{234}U$ and U concentrations of the three measured Siberian Rivers. The more southward Stations 1 and 11 (near Svalbard) suggest that the fresh water component is predominantly ice melt. Two samples appear to have elevated U concentrations with respect to $\delta^{234}U$ and the mixing lines of Yenisey–SW (Leg II Station 20) and ice melt–SW (Leg II Station 1). The reason for this is not clear, but it may be an artefact caused by evaporation of these particular samples during storage prior to the U concentration measurements.

concentration (~2% higher than anticipated). The cause of these enrichments is not clear (see Fig. 6).

The very good agreement between the northern part of the Leg II transect and Makarov Basin samples and the Yenisey–SW river mixing line suggests that the freshwater input into the basin is (1) dominated by a component of Yenisey River origin and (2) is behaving conservatively, transporting ~100% of its U into the interior basin. Transport of riverine waters into the central Arctic Ocean has been documented previously (Guay et al., 2001), although in contrast to this study, inputs from individual rivers could not be reliably separated. Because the Yenisey River has both the highest U concentration and δ^{234}U of all of the Siberian Rivers measured in this study, its signature can be resolved clearly in our dataset; any contribution from the other rivers, or U loss in the estuary/shelf area, would shift the measured compositions away from the SW–Yenisey mixing line and towards lower δ^{234}U compositions (Fig. 4).

While the Ob might be expected to provide a considerable fraction of the freshwater contributions to this area in the Arctic Ocean, this appears to be incompatible with the δ^{234}U and U concentration data. Although it is possible that the river analyses included here do not accurately represent the composition of the river water components seen in the central Arctic Ocean, it is unlikely that the rivers were substantially different and yet when mixed would result in a composition that matches the Yenisey River measurement.

The seawater U concentration and δ^{234}U data suggest that there are no significant inputs from either ice meltwater or from the major rivers, Ob or Lena, entering the central Arctic Ocean sample locations at the time of sampling. Thus, U concentration data, coupled to high-precision δ^{234}U measurements, offers the potential to characterize water mass flow patterns in the central Arctic Ocean. These data also indicate that Yenisey River water flows into the Makarov Basin approximately 1000 km away. Estimates of riverine flow patterns in the Arctic Ocean suggest that the Siberian rivers can penetrate far into the central Arctic Ocean and that this can be achieved on sub-yearly time spans (Karcher and Oberhuber, 2002). For example terrigenous input of organic carbon into the Kara Sea has been reported to be as high as 50% of the total organic carbon even as far away as ~700 km offshore (Krishnamurthy et al., 2001). The apparent lack of an Ob River component in the central Makarov Basin could perhaps be due to a strong steering of the outflow from these two rivers away from each other in the shelf zone at the time of sampling. However, this interpretation is based on the δ^{234}U and U concentration data alone, is speculative and should be verified with independent hydrological evidence.

The Makarov Basin seawaters suggest that the transportation of U from the Yenisey River behaves conservatively, which dramatically contrasts with the non-conservative behaviour observed for the Mackenzie River. Thus, it appears that the rivers have undergone distinct U behaviour in the shelf/estuary zone. In this context, there are some clear differences between the Mackenzie River and the Siberian rivers systems. Specifically, the DOC contents of the Siberian rivers are significantly higher than those present in the Mackenzie River. It is estimated that the DOC present in the Ob and Yenisey Rivers does not experience significant loss before entering the central Arctic Ocean Basins, which contrasts with the appreciable loss of DOC observed in the Canada shelf area (Cooper et al., 2005; Hansell et al., 2004). Thus, if DOC is the primary carrier phase of U, it could explain the differing behaviour between the Mackenzie and Yenisey Rivers. Furthermore, the suspended sediment discharge from the Siberian Rivers is markedly lower than that from the Mackenzie River as well (Holmes et al., 2002), limiting the potential for sediment scavenging of U by Fe-coated phases, from the Yenisey River.

3.4. Implications for the marine U and δ^{234}U budget

Rivers entering the Arctic Ocean contribute about 10% of the total global riverine discharge. The total riverine U flux from the four Arctic rivers measured in this study comprise ~5% of the global riverine U discharge, and due to their elevated δ^{234}U they contribute ~12% of the excess ^{234}U when compared to the compiled global data in Dunk et al. (2002). Thus this may have a significant influence on the global riverine U input and marine δ^{234}U on glacial–interglacial scales, although a thorough investigation of the distribution and behaviour of U covering the entire Arctic Ocean is beyond the scope of this study. The observation of the non-conservative behaviour of U in the Mackenzie River estuary supports the idea of "U storage" in estuaries during interglacials which can be important for variations in the marine δ^{234}U on glacial–interglacial scales (Dunk et al., 2002; Esat and Yokoyama, 2006). Furthermore, the non-conservative U behaviour observed in this study must be taken into account when estimating the total marine U budget as opposed to a general assumption that all riverine U is conservatively transported into the oceans when modelling the marine U budget.

A number of studies have documented both estuarine removal of U from the water column (Swarzenski et al., 2003; McKee et al., 1987; Barnes and Cochran, 1993; Swarzenski and Baskaran, 2006) and U release from underlying sediments (Swarzenski et al., 2003; McKee et al., 1987; Barnes and Cochran, 1993; Swarzenski and Baskaran, 2006) so that the river budgets obtained from freshwater samples must be modified to actually quantify the amount of riverine U that reaches the deep ocean basins. However, since estuarine studies generally cover only limited cross sections of estuarine systems and U modification processes often follow complex patterns, the total net loss (or gain) of U is difficult to quantify. This study demonstrates that high-precision U isotope measurements of waters well beyond the estuary can be used to directly identify and quantify the amount of riverine U that is entering into the deep ocean. Such measurements from other major river systems are required to better characterize the global oceanic U budget.

4. Conclusions

Using high-precision δ^{234}U measurements in river and seawater samples, it is possible to trace distinct riverine inputs into the Arctic Ocean, as well as yield critical information on the behaviour of U during its transportation from rivers into the oceans.

The freshwater source for the less saline surface waters in the central part of the Arctic Ocean can be difficult to assess because several major Siberia Rivers, including the Yenisey, Ob and Lena, can contribute to this. However, less saline seawater samples characterized by elevated δ^{234}U within the Makarov Basin convincingly contain a freshwater component having U concentration and δ^{234}U values that match those of Yenisey freshwater discharge. This indicates that the Yenisey River is the major contributor to the area at the time of sampling, and that significant U losses in the estuarine environment do not occur. This is a significant finding, considering that most studies assume that all rivers are mixing together in the interior of the Arctic Ocean, and offers a more detailed picture of the freshwater budget and flow patterns in the Arctic Ocean. This observation suggests that local steering processes influence the flow patterns for river water masses over the Russian/Siberian shelf area, since the two major rivers, Ob and Yenisey, in close vicinity to each other, appear to have different flow patterns based on the δ^{234}U and U concentration measurements presented in this study.

The Canada Basin obtains a significant freshwater input from the Mackenzie River. Using U concentration and δ^{234}U data, in combination with salinity and δ^{18}O measurements, it can be shown that U transported from the Mackenzie River behaves non-conservatively, losing ~65% of its original U in the estuary/shelf zone before entering the deep areas of the Canada Basin. This is completely different to the apparent conservative behaviour observed for the Yenisey River. The reason for this U removal is not clear, although DOC appears to be transported conservatively across the estuaries of Siberian rivers, while there is substantial net DOC loss in the Mackenzie estuary/shelf zone (Hansell et al., 2004). A likely possibility for the observed U behaviour is that the U is strongly bound to DOC and these are therefore removed together. Furthermore, due to the high sediment flux from the Mackenzie River, U could also be removed by adsorption onto flocculating colloidal organic or Fe phases, as has been observed for other estuary systems (Porcelli et al., 1997, 2001; Andersson et al., 1995, 1998, 2001). The U-bearing phases in the sediment are thereafter scavenged out of the water column.

The new results presented in this study demonstrate unequivocally that the behaviour of U in shelf/estuary systems cannot be generalized and this study demonstrates that waters well beyond the estuary can be used to directly identify and quantify the riverine U that is entering into the deep ocean. This observation is also critically important for the total U budget in the oceans, as it is currently assumed that all riverine U is conservatively transported into the oceans when modelling the marine U budget and can have importance on expected δ^{234}U variations on interglacial–glacial time scales (Chabaux et al., 2003; Dunk et al., 2002; Henderson, 2002; Robinson et al., 2004b; Esat and Yokoyama, 2006; Edwards et al., 2003; Henderson and Anderson, 2003).

Acknowledgments

We are grateful for the valuable support of Felix Oberli, Helen Williams and Sarah Woodland, as well as Urs Menet, Heiri Baur and Bruno Rütsche, and the rest of the IGMR group who expend time and effort to ensure the smooth running of the MC-ICPMS facilities at IGMR. Martin Frank and Bettina Zimmerman are thanked for their extensive efforts in obtaining the samples and providing comments on this work. We thank David Richards for discussions and revisions from two anonymous reviewers. We also thank Jim McClelland, Robert Max Holmes and the PARTNERS project for providing river water samples (the PARTNERS project is mainly funded through grant number

NSF-OPP-0229302). Ship time in the Western Arctic was funded by the US National Science Foundation (NSF-OPP-9996337 to MB). The crew on I/B *Oden* and the Swedish Polar Research Secretariat (SPRS) provided helpful logistical support for the Arctic Ocean 2001 (AO-01) expedition. The project was partly financed by the Swedish Research Council (VR grant #621-2001-2616).

References

Andersen, M.B., Stirling, C.H., Potter, E.K., Halliday, A.N., 2004. Toward epsilon levels of measurement precision on $^{234}U/^{238}U$ by using MC-ICPMS. Int. J. Mass Spectrom. 237, 107–118.

Andersen, M.B., Stirling, C.H., Potter, E.K., Halliday, A.N., Blake, S.G., McCulloch, M.T., Ayling, B.F., O'Leary, M., submitted for publication. Direct chronology of the Marine Isotope Stage 15 (~600 ka) estimated from high-precision U-series ages from Henderson Island, South Pacific, EPSL.

Anderson, L.G., Jutterstrom, S., Kaltin, S., Jones, E.P., Bjork, G.R., 2004. Variability in river runoff distribution in the Eurasian Basin of the Arctic Ocean. J. Geophys. 109.

Andersson, P.S., Wasserburg, G.J., Chen, J.H., Papanastassiou, D.A., Ingri, J., 1995. ^{238}U–^{234}U and ^{232}Th–^{230}Th in the Baltic Sea and in river water. Earth Planet. Sci. Lett. 130, 217–234.

Andersson, P.S., Porcelli, D., Wasserburg, G.J., Ingri, J., 1998. Particle transport of ^{234}U–^{238}U in the Kalix River and in the Baltic Sea. Geochim. Cosmochim. Acta 62, 385–392.

Andersson, P.S., Porcelli, D., Gustafsson, O., Ingri, J., Wasserburg, G.J., 2001. The importance of colloids for the behavior of uranium isotopes in the low-salinity zone of a stable estuary. Geochim. Cosmochim. Acta 65, 13–25.

Barnes, C.E., Cochran, J.K., 1993. Uranium geochemistry in estuarine sediments – controls on removal and release processes. Geochim. Cosmochim. Acta 57, 555–569.

Björk, G., Soderkvist, J., Winsor, P., Nikolopoulos, A., Steele, M., 2002. Return of the cold halocline layer to the Amundsen Basin of the Arctic Ocean: implications for the sea ice mass balance. Geophys. Res. 29.

Borole, D.V., Krishnaswami, S., Somayajulu, B.L.K., 1982. Uranium isotopes in rivers, estuaries and adjacent coastal sediments of western India: their weathering, transport and oceanic budget. Geochim. Cosmochim. Acta 46, 125–137.

Breckel, E., Emerson, S., Balistrieri, L., 2005. Authigenesis of trace metals in energetic tropical shelf environments. Cont. Shelf Res. 25, 1321–1337.

Chabaux, F., Riotte, J., Clauer, N., France-Lanord, C., 2001. Isotopic tracing of the dissolved U fluxes of Himalayan rivers: Implications for present and past U budgets of the Ganges–Brahmaputra system. Geochim. Cosmochim. Acta 65, 3201–3217.

Chabaux, F., Riotte, J., Dequincey, O., 2003. U–Th–Ra fractionation during weathering and river transport, Uranium-Series Geochemistry. Rev. Mineral. Geochem. 52, 533–576.

Chen, J.H., Edwards, R.L., Wasserburg, G.J., 1986. ^{238}U, ^{234}U and ^{232}Th in seawater. Earth Planet. Sci. Lett. 80, 241–251.

Cheng, H., Edwards, R.L., Hoff, J., Gallup, C.D., Richards, D.A., Asmerom, Y., 2000. The half-lives of uranium-234 and thorium-230. Chem. Geol. 169, 17–33.

Cooper, L.W., Benner, R., McClelland, J.W., Peterson, B.J., Holmes, P.M., Raymond, P.A., Hansell, D.A., Grebmeier, J.M., Codispoti, L.A., 2005. Linkages among runoff, dissolved organic carbon, and the stable oxygen isotope composition of seawater and other water mass indicators in the Arctic Ocean. J. Geophys. 110.

Cutler, K.B., Gray, S.C., Burr, G.S., Edwards, R.L., Taylor, F.W., Cabioch, G., Beck, J.W., Cheng, H., Moore, J., 2004. Radiocarbon calibration and comparison to 50 kyr BP with paired ^{14}C and ^{230}Th dating of corals from Vanuatu and Papua New Guinea. Radiocarbon 46, 1127–1160.

Delanghe, D., Bard, E., Hamelin, B., 2002. New TIMS constraints on the uranium-238 and uranium-234 in seawaters from the main ocean basins and the Mediterranean Sea. Mar. Chem. 80, 79–93.

Dittmar, T., Kattner, G., 2003. The biogeochemistry of the river and shelf ecosystem of the Arctic Ocean: a review. Mar. Chem. 83, 103–120.

Dunk, R.M., Mills, R.A., Jenkins, W.J., 2002. A reevaluation of the oceanic uranium budget for the Holocene. Chem. Geol. 190, 45–67.

Edmonds, H.N., Moran, S.B., Cheng, H., Edwards, R.L., 2004. ^{230}Th and ^{231}Pa in the Arctic Ocean: implications for particle fluxes and basin-scale Th/Pa fractionation. Earth Planet. Sci. Lett. 227, 155–167.

Edwards, R.L., Gallup, C.D., Cheng, H., 2003. Uranium-series dating of marine and lacustrine carbonates, Uranium-Series Geochemistry. Rev. Mineral. Geochem. 52, 363–405.

Ekwurzel, B., Schlosser, P., Mortlock, R.A., Fairbanks, R.G., Swift, J.H., 2001. River runoff, sea ice meltwater, and Pacific water distribution and mean residence times in the Arctic Ocean. J. Geophys. Res. [Oceans] 106, 9075–9092.

Esat, T.M., Yokoyama, Y., 2006. Variability in the uranium isotope composition of the oceans over glacial–interglacial time scales. Geochim. Cosmochim. Acta 70, 4140–4150.

Guay, C.K.H., Falkner, K.K., Muench, R.D., Mensch, M., Frank, M., Bayer, R., 2001. Wind-driven transport pathways for Eurasian Arctic river discharge. J. Geophys. Res. [Oceans] 106, 11469–11480.

Hamelin, B., Bard, E., Zindler, A., Fairbanks, R.G., 1991. $^{234}U/^{238}U$ mass-spectrometry of corals – how accurate is the U–Th age of the last interglacial period. Earth Planet. Sci. Lett. 106, 169–180.

Hansell, D.A., Kadko, D., Bates, N.R., 2004. Degradation of terrigenous dissolved organic carbon in the western Arctic Ocean. Science 304, 858–861.

Hart, S.R., Zindler, A., 1989. Isotope fractionation laws – a test using calcium. Int. J. Mass Spectrom. Ion Process. 89, 287–301.

Henderson, G.M., 2002. Seawater ($^{234}U/^{238}U$) during the last 800 thousand years. Earth Planet. Sci. Lett. 199, 97–110.

Henderson, G.M., Anderson, R.F., 2003. The U-series toolbox for paleoceanography. Uranium-Series Geochem. Rev. Mineral. Geochem. 52, 493–531.

Holmes, R.M., McClelland, J.W., Peterson, B.J., Shiklomanov, I.A., Shiklomanov, A.I., Zhulidov, A.V., Gordeev, V.V., Bobrovitskaya, N.N., 2002. A circumpolar perspective on fluvial sediment flux to the Arctic Ocean. Glob. Biogeochem. 16.

Karcher, M.J., Oberhuber, J.M., 2002. Pathways and modification of the upper and intermediate waters of the Arctic Ocean. J. Geophys. 107.

Kigoshi, K., 1971. Alpha-Recoil thorium-234 – dissolution into water and uranium-234/Uranium-238 disequilibrium in nature. Science 173, 47.

Klinkhammer, G.P., Palmer, M.R., 1991. Uranium in the oceans: where it goes and why. Geochim. Cosmochim. Acta 55, 1799–1806.

Krishnamurthy, R.V., Machavaram, M., Baskaran, M., Brooks, J.M., Champ, M.A., 2001. Organic carbon flow in the Ob, Yenisey

Rivers and Kara Sea of the Arctic Region. Mar. Pollut. Bull. 42, 726–732.

Ku, T.L., Knauss, K.G., Mathieu, G.G., 1977. Uranium in open ocean – concentration and isotopic composition. Deep-Sea Res. 24, 1005–1017.

Luo, X.Z., Rehkämper, M., Lee, D.C., Halliday, A.N., 1997. High precision $^{230}Th/^{232}Th$ and $^{234}U/^{238}U$ measurements using energy-filtered ICP magnetic sector multiple collector mass spectrometry. Int. J. Mass Spectrom. 171, 105–117.

Macdonald, R.W., Solomon, S.M., Cranston, R.E., Welch, H.E., Yunker, M.B., Gobeil, C., 1998. A sediment and organic carbon budget for the Canadian Beaufort Shelf. Mar. Geol. 144, 255–273.

Macdonald, R.W., Carmack, E.C., McLaughlin, F.A., Falkner, K.K., Swift, J.H., 1999. Connections among ice, runoff and atmospheric forcing in the Beaufort Gyre. Geophys. Res. Lett. 26, 2223–2226.

Mann, D.K., Wong, G.T.F., 1993. Strongly bound uranium in marine waters – occurrence and analytical implications. Mar. Chem. 42, 25–37.

McKee, B.A., Demaster, D.J., Nittrouer, C.A., 1987. Uranium geochemistry on the amazon shelf – evidence for uranium release from bottom sediments. Geochim. Cosmochim. Acta 51, 2779–2786.

Nghiem, S.V., Chao, Y., Neumann, G., Li, P., Perovich, D.K., Street, T., Clemente-Colon, P., 2006. Depletion of perennial sea ice in the East Arctic Ocean. Geophys. Res. Lett. 33. doi:10.1029/2006GL027198.

Overpeck, J.T., Sturm, M., F.J.A., S.M.C., Benner, R., Carmack, E.C., Chapin III, F.S., Gerlach, S.C., Hamilton, L.C., Hinzman, L.D., Holland, M., Huntington, H.P., Key, J.R., Lloyd, A.H., MacDonald, G.M., MacFadden, J., Noone, D., Prowse, T.D., Schlosser, P., Vörösmarty, C., 2005. Arctic system on trajectory to new, seasonally ice-free state. EOS Trans. AGU 86, 309–313.

Palmer, M.R., Edmond, J.M., 1993. Uranium in river water. Geochim. Cosmochim. Acta 57, 4947–4955.

Peterson, B.J., Holmes, R.M., McClelland, J.W., Vorosmarty, C.J., Lammers, R.B., Shiklomanov, A.I., Shiklomanov, I.A., Rahmstorf, S., 2002. Increasing river discharge to the Arctic Ocean. Science 298, 2171–2173.

Porcelli, D., Andersson, P.S., Wasserburg, G.J., Ingri, J., Baskaran, M., 1997. The importance of colloids and mires for the transport of uranium isotopes through the Kalix River watershed and Baltic Sea. Geochim. Cosmochim. Acta 61, 4095–4113.

Porcelli, D., Andersson, P.S., Baskaran, M., Wasserburg, G.J., 2001. Transport of U- and Th-series nuclides in a Baltic Shield watershed and the Baltic Sea. Geochim. Cosmochim. Acta 65, 2439–2459.

Potter, E.K., Stirling, C.H., Andersen, M.B., Halliday, A.N., 2005. High precision Faraday collector MC-ICPMS thorium isotope ratio determination. Int. J. Mass Spectrom. 247, 10–17.

Robinson, L.F., Belshaw, N.S., Henderson, G.M., 2004a. U and Th concentrations and isotope ratios in modern carbonates and waters from the Bahamas. Geochim. Cosmochim. Acta 68, 1777–1789.

Robinson, L.F., Henderson, G.M., Hall, L., Matthews, I., 2004b. Climatic control of riverine and seawater uranium-isotope ratios. Science 305, 851–854.

Schlosser, P., Kromer, B., Ostlund, G., Ekwurzel, B., Bonisch, G., Loosli, H.H., Purtschert, R., 1994a. On the C-14 and Ar-39 distribution in the central Arctic-Ocean – implications for deep-water formation. Radiocarbon 36, 327–343.

Schlosser, P., Bauch, D., Fairbanks, R., Bonisch, G., 1994b. Arctic river-runoff – mean residence time on the shelves and in the halocline. Deep-Sea Res. Part 1, Oceanogr. Res. Pap. 41, 1053–1068.

Schlosser, P., Swift, J.H., Lewis, D., Pfirman, S.L., 1995. The role of the large-scale Arctic Ocean circulation in the transport of contaminants. Deep-Sea Res., Part 2, Top. Stud. Oceanogr. 42, 1341–1367.

Stirling, C.H., Potter, E.-K., Andersen, M.B., Halliday, A.N., Spötl, C., 2003. Isotope fractionation of uranium in low-temperature environments. EOS Trans. AGU 84 (Abstract V11H-02).

Stirling, C.H., Halliday, A.N., Porcelli, D., 2005. In search of live ^{247}Cm in the early solar system. Geochim. Cosmochim. Acta 69, 1059–1071.

Stirling, C.H., Halliday, A.N., Potter, E.-K., Andersen, M.B., Zanda, B., 2006. A low initial abundance of ^{247}Cm in the early solar system: implications for r-process nucleo-synthesis. Earth Planet. Sci. Lett. 251, 386–397.

Stirling, C.H., Andersen, M.B., Potter, E.-K., Halliday, A.N., in press. Isotope fractionation of $^{235}U/^{238}U$ in low-temperature environments, Earth Planetary Scientific Letters.

Swarzenski, P.W., Baskaran, M., 2006. Uranium distribution in the coastal waters and pore waters of Tampa Bay, Florida. Mar. Chem. 102, 252–266.

Swarzenski, P.W., McKee, B.A., Booth, J.G., 1995. Uranium geochemistry on the amazon shelf – chemical-phase partitioning and cycling across a salinity gradient. Geochim. Cosmochim. Acta 59, 7–18.

Swarzenski, P.W., Porcelli, D., Andersson, P.S., Smoak, J.M., 2003. The behavior of U- and Th-series nuclides in the estuarine environment. Uranium-Series Geochem. Rev. Mineral. Geochem. 52, 577–606.

Swarzenski, P., Campbell, P., Porcelli, D., McKee, B., 2004. The estuarine chemistry and isotope systematics of $^{234,238}U$ in the Amazon and Fly Rivers. Cont. Shelf Res. 24, 2357–2372.

Trimble, S.M., Baskaran, M., Porcelli, D., 2004. Scavenging of thorium isotopes in the Canada Basin of the Arctic Ocean. Earth Planet. Sci. Lett. 222, 915–932.

Vigier, N., Bourdon, B., Turner, S., Allegre, C.J., 2001. Erosion time scales derived from U-decay series measurements in rivers. Earth Planet. Sci. Lett. 193, 549–563.